Review

Nanostructured transition metal nitrides for energy storage and fuel cells

Shanmu Dong, Xiao Chen, Xiaoying Zhang, Guanglei Cui *

Qingdao Institute of Bioenergy and Bioprocess Technology, Chinese Academy of Sciences, Qingdao 266101, PR China

Contents

ARTICLE INFO

ABSTRACT

The research of advanced electrodes for energy storage and energy conversion has been an important strategy to satisfy the ever increasing need for future electrochemical power sources. In this review, we describe the recent studies on the preparation and application of nanostructured transition metal nitrides as alternative electrode materials. We also highlight the design of nanostructured materials needed to balance the electronic and ionic conduction, which are of great importance for achieving enhanced performance of electrode in electrochemical devices. By providing this brief survey, we aim to illustrate that transition metal nitrides with proper nanostructure would result in improved electrochemical performance of electrode materials in energy storage and conversion applications.

1. Introduction

The ever increasing demand for clean energy, such as wind, solar, and tidal power has stimulated great interest in electrochemical energy conversion and storage. To meet the requirements for future electrochemical power sources, it is urgent to explore advanced electrodes with well-controlled nanostructure for dramatic enhancements of energy and power density, catalytic activity, efficiency, and durability. Therefore, the need for alternative, abundant, and financially feasible electrode materials becomes more urgent. This global challenge has provided excellent opportunities for materials chemistry in the design and exploration of new materials.

Among solid-state compounds and materials, oxides are by far the most ubiquitous, most extensively studied, and best characterized. As compared to oxides, nitrides are also versatile compounds that formed with most of the periodic table components, especially many metals. A convenient way of classifying nitrides is in terms of their bonding [1]. (i) The Group I and Group II metals that form nitrides generate compounds that contain essentially ionic bonds. In this bonding category, for instance, lithium forms an ionic nitride of formula Li_3N, which exhibits excellent ionic conductivity [2,3]. (ii) Elements in Groups III and IV form covalently bonded nitrides. They are generally non-conductive or semi-conductive with high degrees of hardness and high melting points [4]. (iii) The bonding in transition metal nitrides can be described as simultaneous contributions from metallic, covalent, and ionic bonding, which endow them unique physical and chemical properties [5–9]. In this review, we focus on the application of transition metal nitrides in the exploration of novel electrode materials for electrochemical energy storage and fuel cell applications.

* Corresponding author. Tel.: +86 532 80662746; fax: +86 532 80662744.
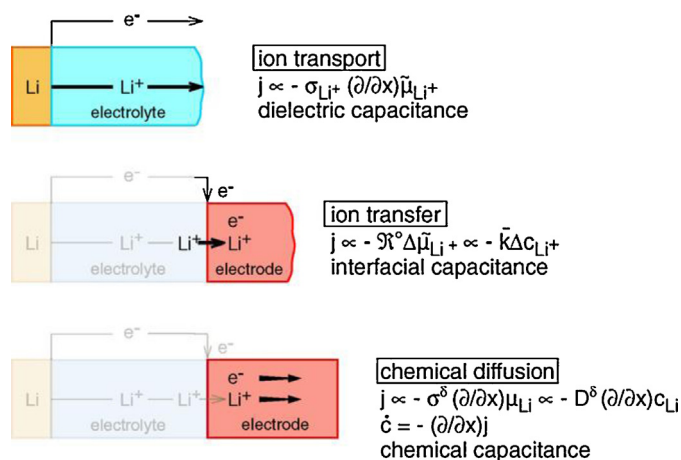E-mail address: cuigl@qibebt.ac.cn (G. Cui).

Fig. 1. Three dynamic processes for lithium ions transportation in Li-ion battery systems.
Figure was reproduced from Ref. [17], with permission of the copyright holders.
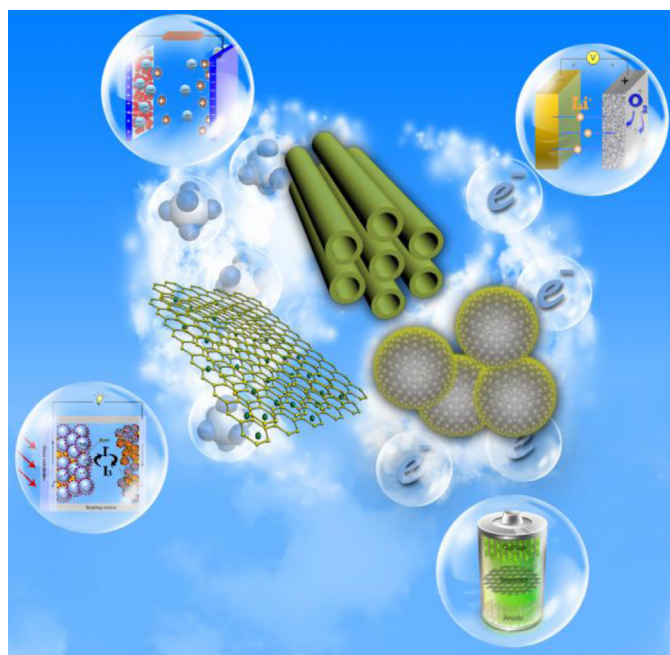

Fig. 2. Schematic of nanostructured materials with optimized ionic and electronic conductivity for electrochemical energy conversion and storage devices.

The formation of transition metal nitrides modifies the nature of the *d*-band of the parent metal, resulting in a contraction of the metal *d*-band. Such a *d*-band contraction would cause a greater density of states (DOS) near the Fermi level in comparison with the parent metal [10]. The redistributions of the DOS in transition metal nitrides give rise to their attractive catalytic activities, which are different from those of the parent metals but similar to those of group VIII noble metals [11,12]. From the structural point of view, the introduction of nitrogen into the lattice of the early transition metals results in an increase of the lattice parameter, corresponding to the enhanced d-electron density. Transition metal nitrides belong to the family of interstitial compounds or alloys. The arrangement of metal atoms in interstitial nitrides is either face centered cubic or hexagonal close-packed. The common features of this class of materials are simple metallic structures with the smaller nitrogen atoms randomly distributed on the interstitial sites [13,14]. These features of structures and bonding endow transition metal nitrides with attractive electronic conductivity, catalytic activity, and optical properties. All these characteristics mentioned above, together with high resistance against corrosion and high melting points, make transition metal nitrides a promising choice for the electrode material of electrochemical devices.

To achieve improved storage capacity and catalytic activity, as the basic interest of electrode materials in such electrochemical systems is mixed conductance. Since the transport of ions in the electrode materials should obey the rule of electroneutrality, compensating electrons simultaneously flow through the outer wire. To reduce the electrode resistance, as proposed by Maier, an ideal electrode material is required to possess both superior electronic and ionic conductivity [15–17].

In the Li-ion battery system, for instance, there are three dynamic processes for Li$^+$ transportation: (i) Li$^+$ motion through the electrolyte accompanied by electron flowing in the outer circuit; (ii) interfacial ion transfer; (iii) chemical diffusion accompanied by electron in the bulk of electrode material, as shown in Fig. 1. In processes (iii), the driving force of ambipolar diffusion (Li$^+$ and electron) is expressed in terms of Li concentration gradients, which can be defined as the function: $\tau = L^2/2D$, where τ is the diffusion time, L is the length of diffusion path and D is diffusion coefficient of the electrode material. Consequently, a low conductivity in the active material is compensated by a short conduction path. Compared to micrometer-sized materials, nanoscale materials shorten the diffusion length of Li$^+$ in the electrode, resulting in dramatically improved ionic conductance [17]. Therefore, nanosized electrode materials have the genuine potential to make a significant improvement on the performance of electrode materials. However, as for nanoparticles, the enlarged electrolyte/electrode surface area may lead to significant side reactions, especially decomposing carbonate solvent, on the interfaces and consequently bring forth potential safety events [18–20]. Therefore, it is desirable to design optimized nano-structured electrode materials with superior mixed (electron and ion) conduction for electrochemical energy conversion and storage applications [21] (Fig. 2).

Herein, in this review, we will firstly present the recent reports on the preparation of nanostructured transition metal nitride materials. In the following sections, some recent research developments in electrochemical energy storage and energy conversion (especially electrochemical catalysis for fuel cell) applications will be described. The strategy of mixed (ionic and electronic) conduction in the design of these nanostructured transition metal nitrides for electrochemical devices is highlighted.

2. The preparation of nanostructured transition metal nitrides

Although transition metal nitrides have drawn considerable attention in a wide range of applications, there are still limited strategies to prepare nanostructured nitrides on a scalable pathway. Generally speaking, the synthetic strategy of transition metal nitrides can be divided into physical and chemical approaches [22]. Among physical approaches, physical vapor deposition [23,24], plasma and laser methods [25,26] are most involved, which commonly result in defined structure. However, these processes can be only applied to synthesize a few restricted varieties of products, such as TiN and CrN. On the other hand, the chemical approaches involve reactions of parental metals, corresponding metal oxides or any suitable metal precursor with nitrogen sources (such as ammonia or nitrogen) at high temperature (from 800 °C up to 2000 °C) [27–33]. These processes are more versatile with a broader range of nitrides and have been widely used in scientific explorations. Among them, Kumta et al. presented a strategy involving metal alkoxide reaction with large excess of hydrazine to obtain powders and subsequently annealing in Ar atmosphere.
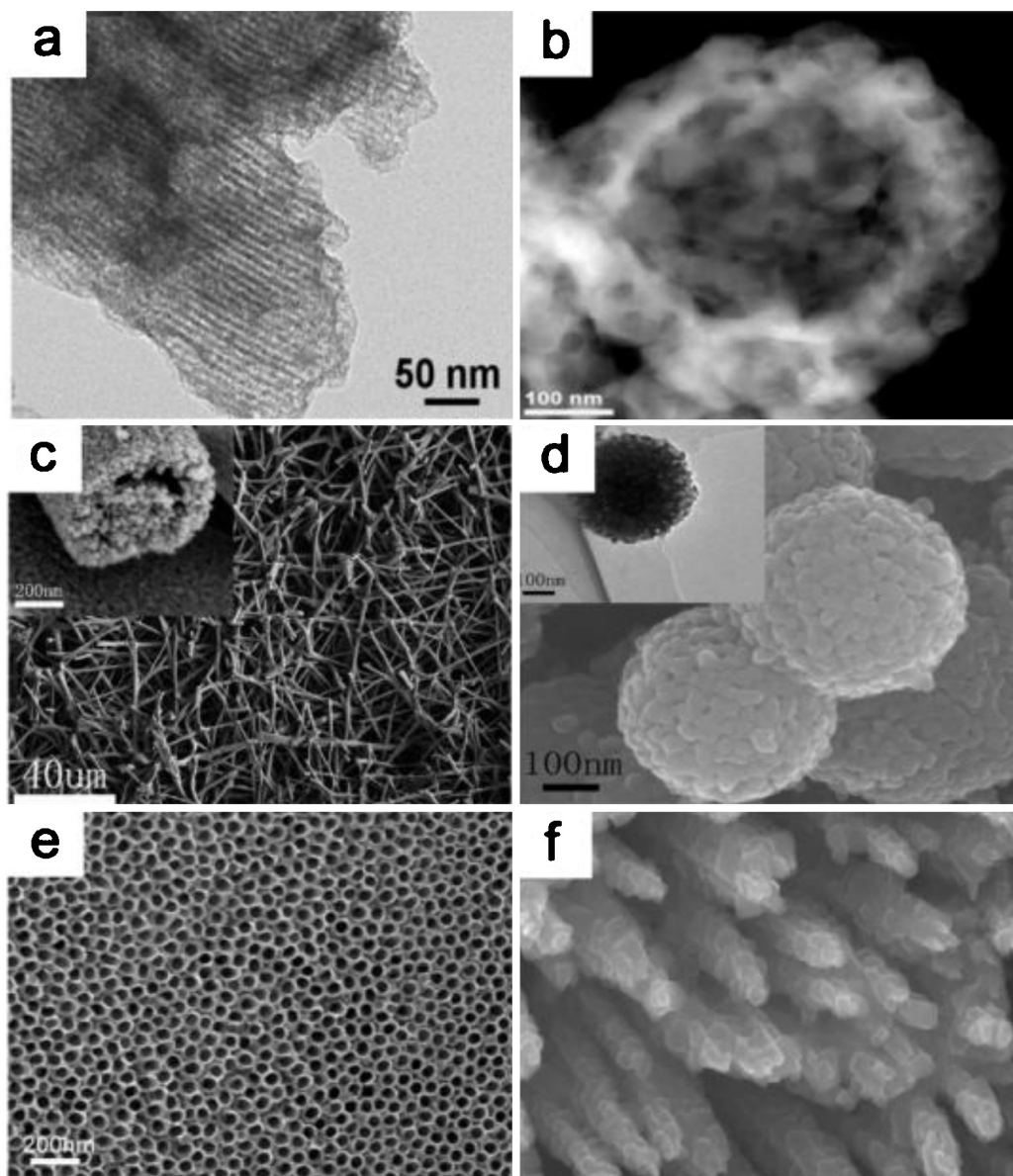
Fig. 3. Nanostructured transition metal nitrides: (a) mesoporous TiN; (b) hollow TiN mesoporous spheres; (c) VN–TiN coaxial mesoporous fibers; (d) TiN mesoporous spheres; (e) TiN nanotube arrays; (f) TiN nanorod arrays.

Figure was reproduced from Refs. [38,42–46], with permission of the copyright holders.

In their study, for instance, nanocrystalline TiN of about 15 nm was obtained [34]. Antonietti and co-workers use cyanamide or urea as nitrogen source and a structural confinement to synthesize a series of transition metal nitrides (TiN, VN, NbN, GaN, Mo$_2$N, W$_2$N, CrN) nanoparticles [35–37]. However, the chemical methods are challenging to achieve nanostructured morphology, such as hierarchically mesoporous structure, because of the aggregation of nanoparticles at high temperature and the collapse of the nanopores during conversion and recrystallizaion.

To address this issue, several feasible synthetic methods have been applied for preparing nanostructured transition metal nitrides. As to the preparation of mesoporous nitrides, the general synthetic strategies have mostly relied on the use of sacrifice templates [38–40,35,41,42]. For instance, Antonietti and co-workers have reported mesoporous titanium nitride/carbon composite with 2D hexagonal symmetry using SBA-15ht and carbon nitride as multiple sacrifice templates (Fig. 3a) [38]. However, these strategies require a tedious and time consuming process of templates preparation and removal. Recently, Cui et al. have reported a facile route

to directly convert TiO$_2$ mesoporous spheres into TiN mesoporous spheres using cyanamide to retain the morphology (Fig. 3d) [43]. In the following study, they reported the fabrication of mesoporous fiber of TiN–VN coxial electrospinning fibers with Polyvinylpyrrolidone, tetrabutyl titanate, and vanadium (III) acetylacetonate as precursors (Fig. 3c) [44]. Furthermore, their group has fabricated the one-dimensional nanoarrays (both nanotube and nanowire) of TiN material (Fig. 3e and f) [45,46]. In these processes, one dimensional TiN nanoarrays were obtained by converting TiO$_2$ arrays using ammonia annealing at high temperature, where the slow heating ramp of temperature was critical for successful preparation.

3. Transition-metal nitrides for electrochemical energy storage

Li-ion battery and supercapacitors are among the most widely explored rechargeable energy storage devices. Li-ion battery

Table 1
A summarization of the theoretical capacity, experimental capacity and the calculated Gibbs free energy [59]: the classification of complete conversion and partial conversion of transition metal nitrides is based on their reported reaction mechanisms.

		Theoretical capacity (mAh g^{-1})	Experimental capacity (mAh g^{-1})	$\Delta_r G$ (kJ mol^{-1})	Reference
Complete conversion	CrN	1218	1200	−35.6	[56]
	Mn$_3$N$_2$	567.2	579	–	[64]
	Fe$_3$N	443	420	–	[58]
	Co$_3$N	421	340	−31.4	[58]
	Ni$_3$N	422	410	–	[57]
	Zn$_3$N$_2$	717.3	555	−98.8	[54]
Partial conversion	VN	1218.2	140	62.5	[60]
	Mn$_4$N	343	210	−5.9	[65]
	CoN	1102	990	–	[66]
	TiN	1299.5	120	115.2	

stores energy in the bulk of active materials through lithium intercalation/de-intercalation, while supercapacitor stores charge on the surface of active materials. Generally, the Li-ion battery exhibits promising gravimetric and volumetric energy densities (150 Wh kg^{-1} and 350 Wh L^{-1}, respectively) but limited power capabilities (<1 kW kg^{-1}). On the other hand, supercapacitors have much higher power densities (10 kW kg^{-1}) [47]. However, their energy densities are far lower than the Li-ion battery. To meet the demand for power sources of hybrid-electric (HEVs) and plug-in hybrid-electric vehicles (PHEVs), there is a need for improved devices that can span the performance gaps between Li-ion batteries and supercapacitors [48,49]. A number of researches have heeded the call and explored mixed conducting (electron and ionic) electrode materials based on transition metal nitride nanocomposites.

3.1. Transition-metal nitrides for lithium storage

Series of transition metal nitrides have been studied as anode materials for Li-ion battery applications. Since lithium storage capacity is the key factor of electrode materials, attention has been drawn in the understanding of its reaction mechanism. According to previous reports, most of transition metal nitrides undergo a conversion reaction for Li storage [50–52]. However, different reaction process and even contradictory results on the conversion mechanisms have been reported. In 2000, nitrides were reported to undergo a similar conversion reaction as transition metal oxides [53]. This reaction firstly generates a Li$_3$N matrix and electrochemically active metal. Subsequently, metal alloying and de-alloying reaction with Li provide the reversible capacity. However, in 2002, studies of Amatucci and coworkers [54] suggested that some of the transition metal nitrides, such as Zn$_3$N$_2$, could directly convert into LiZn without transformation into metallic Zn. Furthermore, their group reported the reaction mechanism of Cu$_3$N (Fig. 4) [55], which suggested that Li did not alloy with Cu metal (Fig. 4d). Until now, the Li storage mechanisms of some transition metal nitrides remained elusive.

Among all the nitrides, CrN reported by Fu et al. exhibited the highest reversible capacity of 1200 mAh g^{-1} under the same reaction mechanism of Cu$_3$N (Fig. 5) [56]. This result was much
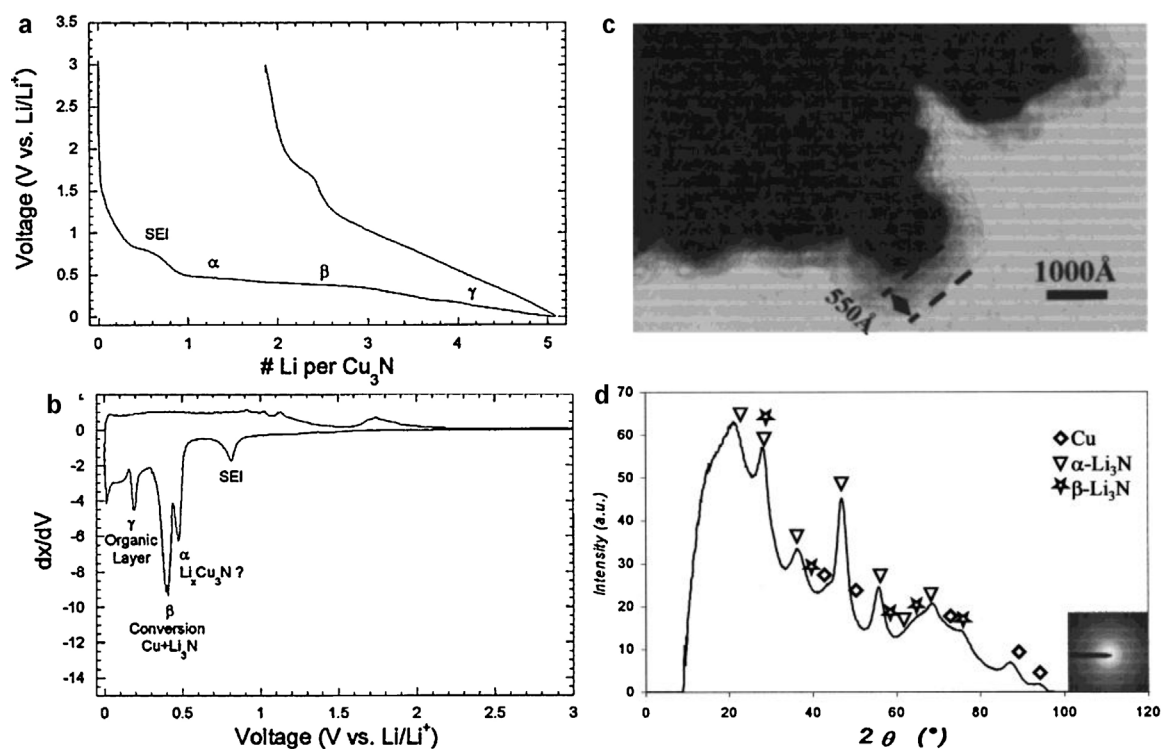

Fig. 4. (a) First cycle voltage profile of a Cu$_3$N electrode cycling vs. Li metal; (b) Corresponding derivative dx/dV plotted vs. voltage; (c) ex situ TEM image of a Cu$_3$N electrode lithiated down to 0 V; (d) the intensity distribution obtained by conversion of the ex situ SAED pattern using process diffraction software. Figure was reproduced from Ref. [55], with permission of the copyright holders.
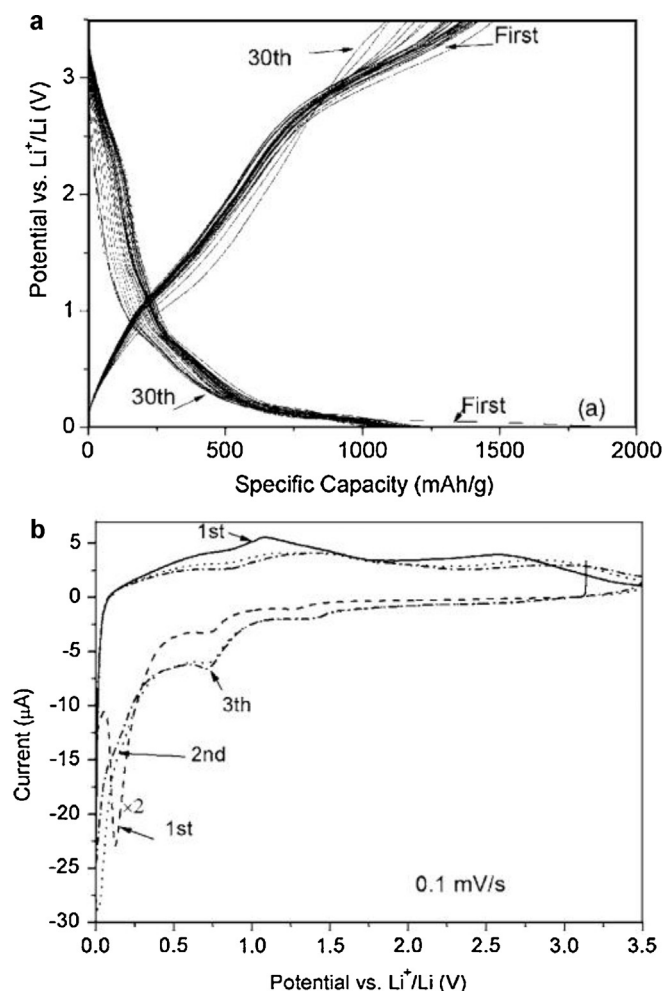
Fig. 5. (a) Charge/discharge cyclic curves of the as-deposited CrN thin film at the current density of 28 $\mu A\,cm^{-2}$; (b) the first three CV profiles of CrN thin films. Figure was reproduced from Ref. [59], with permission of the copyright holders.

higher than other 3d metal of Ni, Fe, Co based nitrides (about 400 mA h g^{-1}) with the same conversion system [57,58]. All of the nitrides mentioned above can deliver a reversible capacity close to the theoretical results provided in the report of Li et al. [59] (Table 1), indicating a complete conversion upon reaction with Li. Interestingly, the values of the Gibbs free energy for these nitrides conversion reaction are negative, which indicate that the reaction along this direction is thermodynamically favorable. Furthermore, it is also worth noting that these high capacities are obtained on nano-sized thin film electrodes. These nano-sized electrodes reduce the diffusion length of Li$^+$ and facilitate the ionic and electronic conduction, which beneficially give rise to the high reversible capacity.

Recent studies suggest that the conversion reactions of some transition metal nitrides are partially limited and cannot achieve their theoretical capacities. Cui et al. have reported a partial conversion reaction of VN nanoparticles supported by nitrogen-doped graphene nanosheet [60]. A gradual increase of reversible capacity during charge/discharge cycles was observed (Fig. 6a). XRD analysis revealed a shift of electrochemically reformed "VN" peaks toward larger angles (with respect to the initial VN phase), corresponding to a lattice contraction after cycling (Fig. 6b). However, no vanadium metal was detected at the end of lithiation. These results may be attributed to the formation of a Li$_x$V$_{1-x}$N phase. Electron energy-loss spectroscopy (EELS) analysis are conducted to detect

the chemical changes of VN after cycling, which illustrate that lithium is partially and gradually incorporated into the lattice of VN resulting in smaller and thinner nanoparticles (Fig. 6d). It is worth noting that the value of $\Delta_r G$ for VN is positive (reported by Li et al., Table 1), indicating that the reaction along this direction is unfavorable. Therefore, the conversion reaction of VN nanoparticles may be limited to some extent. Up to date, the clear reasons still required further exploration.

As mentioned above, the reported CrN, Cu$_3$N can obtain high capacity on a nanosized thin film electrode. However, the rate capability of these materials still needs further improvement. On the other hand, TiN material was reported to possess the metallic characteristics with a good electronic conductivity due to its bonding scheme [34,61]. However, our study suggested that the conversion reaction of Li storage could hardly take place in the case of TiN materials (unpublished results) probably due to the unfavorable positive $\Delta_r G$ value (Table 1). In the meanwhile, metal nitrides have a good tendency to form solid state solution. Therefore, TiN based nanostructured composites are expected to provide highly efficient mixed (electron and Li$^+$) conducting network and optimized electrode interface, which are crucial for high energy density, high power density Li-ion batteries. By collaborating with Prof. J. Maier and Prof. M. Antonietti from Max-Plank Institute, Cui et al. explore a Ti–V–N/C nanocomposite (Fig. 7) [62]. The obtained Ti–V–N/C composite with a particle size of 8 nm exhibits good rate performance with the capacity of 95 mA h g^{-1}, at the rate 22.32 A g^{-1}. Furthermore, TiN was also involved as an electronically conductive addition in graphene/TiN to enhance the vertical electronic conductivity of this hybrid material (Fig. 8) [63]. At a current density of 2000 mA g^{-1}, the capacity of hybrid anode still retains 325 mA h g^{-1} while that of graphene electrode is only 98 mA h g^{-1} (Fig. 8b).

3.2. Transition-metal nitrides for charge Storage in supercapacitor applications

Recent studies of psuedocapacitors are focused on finding a cheaper alternative to ruthenium oxide. Transition metal nitrides like VN [33,67–72], TiN [34], WN [73], MoNx [74], and Co$_3$Mo$_3$N [75] have been studied as alternative candidates because of their low cost and high chemical resistance. Among various options, VN has been reported to deliver 1340 F g^{-1} [67]. However, subsequent studies by the same group reported more modest capacitance values of 160 F g^{-1} for nanocrystalline VN synthesized nominally in the same manner, which suggested that the capacitance may be related to the surface state of electrode material [68]. Furthermore, as proposed by Kumta et al., the estimated conductivity of nanoparticles was 2–3 fold smaller than that of a bulk material, resulting in a limited rate capability. Therefore, an appropriate nanostructure involving nanosize active species with electronically conductive framework has to be designed. As mentioned above, nanostructured TiN with good electric conductivity can serve as a promising electronic conducting framework. Accordingly, TiN–VN fibers of core–shell structures were prepared by the coaxial electro-spinning, and subsequently annealed in the ammonia (Fig. 9) [44]. TiN–VN fibers incorporated mesoporous structure into mixed conducting transition nitride hybrids, which exhibits high specific capacitance (2 mV s^{-1}, 247.5 F g^{-1}) and good rate capability (50 mV s^{-1}, 160.8 F g^{-1}).

Furthermore, one dimensional nanostructured coaxial composite of MnO$_2$ and TiN is designed, which is based on the concept of designing an efficient, fast charge transportation network (Fig. 10) [46]. The combination of mesoporous MnO$_2$ and TiN in coaxial nanowire arrays has shown promising capacitance (390.2 F g^{-1} at a current density of 400 A g^{-1}), excellent rate capability (only 45% loss at a scan rate of 2000 mV s^{-1} compared with that of 2 mV s^{-1}).
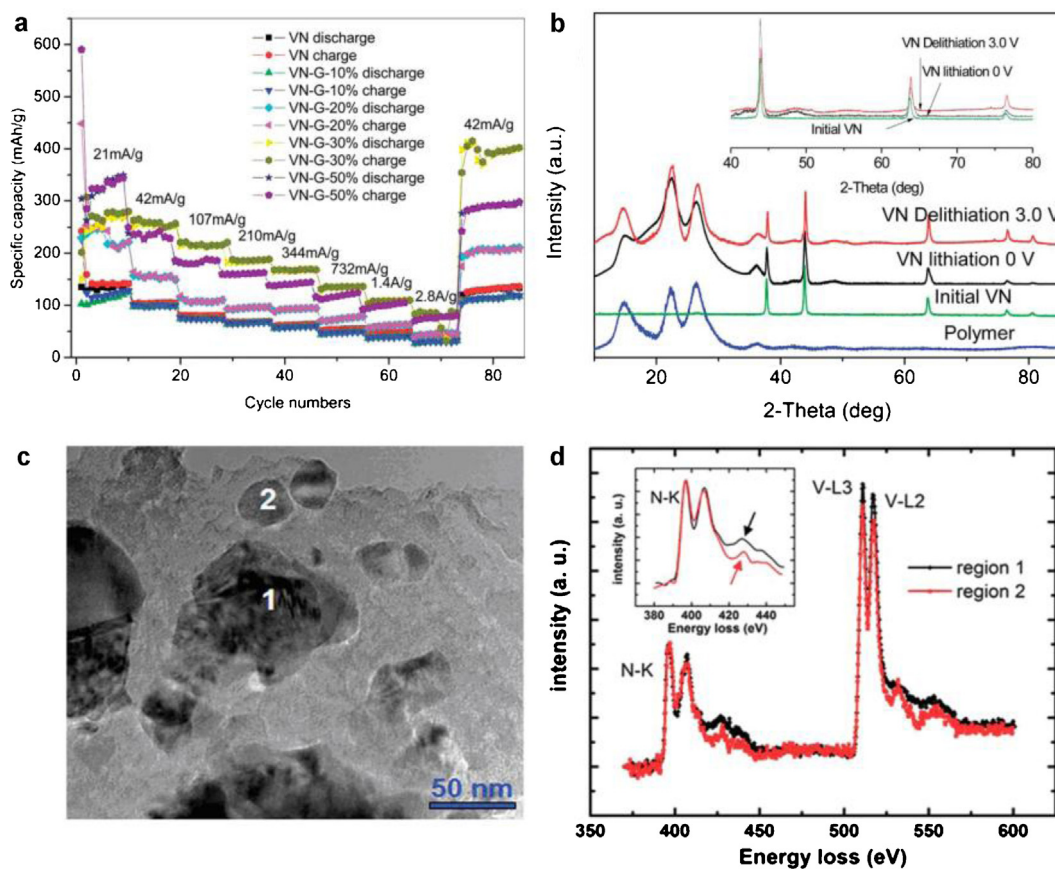
Fig. 6. (a) Cycling and rate performance of VN/graphene hybrid materials and pristine VN electrodes; (b) XRD patterns of the VN electrode obtained at the end of lithiation at 0 V and at the end of delithiation at 3.0 V compared to the initial VN electrode. (c) TEM and (d) EELS analysis of the VN/graphene samples indicating that lithium ions are incorporated into the vanadium nitride by extended cycling.

Figure was reproduced from Ref. [60], with permission of the copyright holders.

To further improve the energy density of supercapacitors, an effective approach is to increase the working voltage of the system, which is only about 1.3 V for aqueous electrolyte supercapacitors and 2.5–2.7 V for conventional EDLCs [76]. Therefore, substantial researches have been carried out to develop "Li-ion capacitors" with higher working voltage [77–79]. Recently, Jang et al. have

reported a new system based on the exchange of lithium ions between the surfaces of two nanostructured electrodes, which exhibited, impressive energy density (160 Wh kg$^{-1}_{cell}$) as well as a promising power density (10 kW kg$^{-1}_{cell}$) [80]. Our researches have demonstrated that metal nitrides may also serve as alternative electrode materials for this novel device [43]. We have introduced TiN
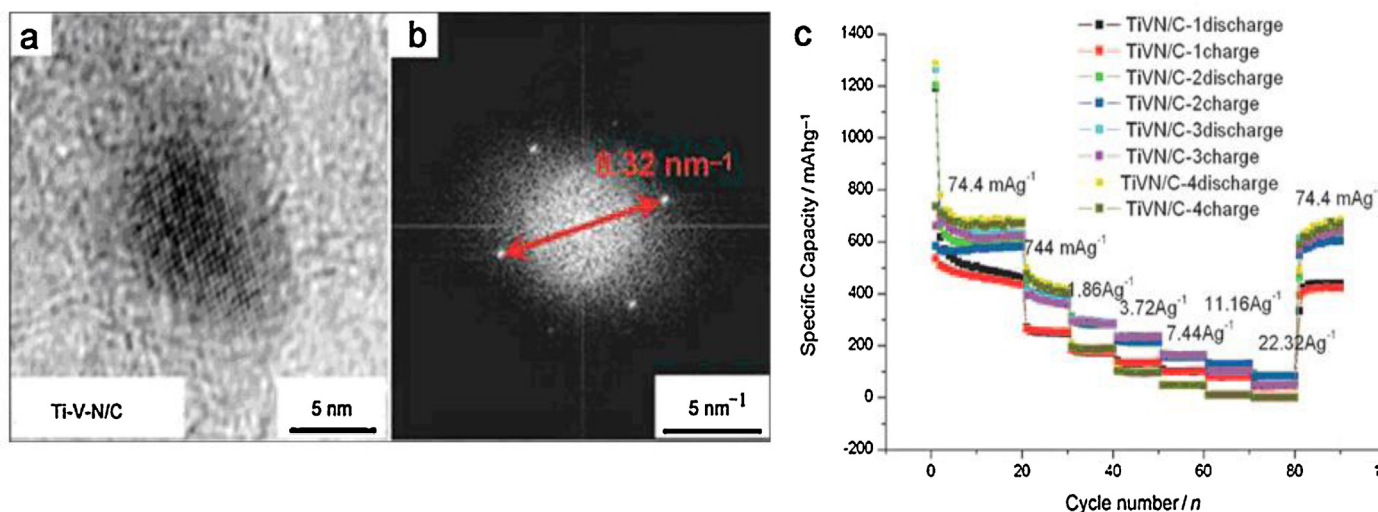

Fig. 7. (a) High revolution TEM image, (b) electron diffraction pattern, and (c) cycling and rate performance of Ti–V–N/C nanocomposite.

Figure was reproduced from Ref. [62], with permission of the copyright holders.
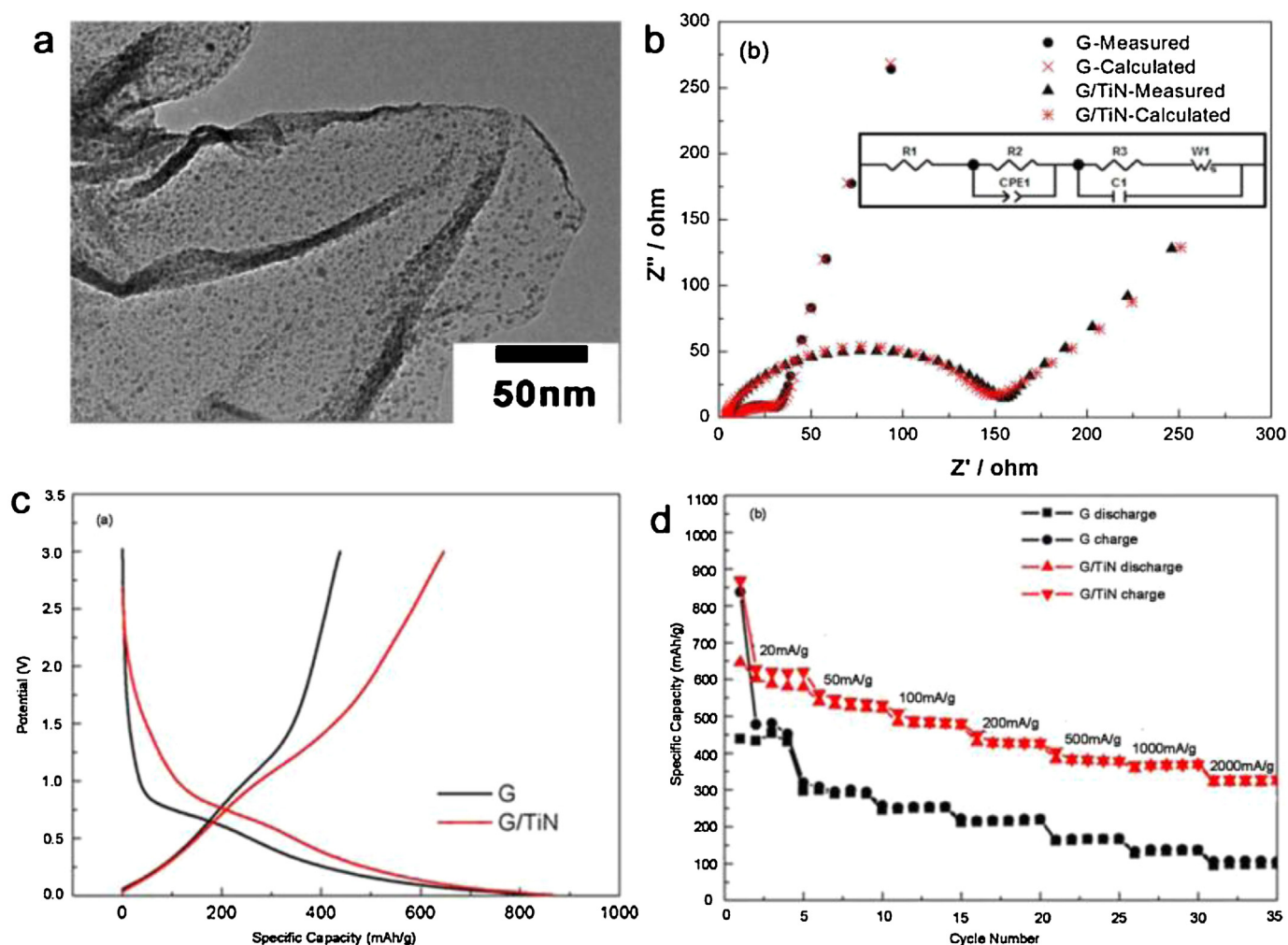
Fig. 8. (a) First charge/discharge profiles of graphene/TiN and graphene at the current density of 20 mA g^{-1}; (c) rate performance of graphene/TiN and graphene. Figure was reproduced from Ref. [63], with permission of the copyright holders.

mesoporous spheres as the electrodes of Li-ion capacitors (Fig. 11). Which can deliver a high single-electrode specific capacitance of 112.3 F g^{-1} at the current densities of 0.1 A g^{-1}. The energy density of this system can reach 45.0 Wh kg^{-1} at a power density of 150 W kg^{-1}.

4. Transition metal nitrides for electrocatalysts

As mentioned in Section 1, the introduction of nitrogen into the lattice of the early transition metals leads to an increase in the d-electron density. The filled states of d-band are narrowed after formation of nitrides, resulting in a similar electronic structure with noble metals up to the Fermi level. Therefore, transition-metal nitrides have evolved a potential candidate for the noble metal material catalyst. In the following section, the application of these materials in electrochemical catalysis, especially for oxygen reduction in fuel cell and Li-air batteries, will be described for substitution of Pt materials.

4.1. Transition metal nitrides for the catalysis of I_3^-/I^-

Dye-sensitized solar cells (DSCs) have evolved a potential candidate for the next generation solar cells owing to their low cost, easy fabrication and respectable efficiency to convert solar energy into

Table 2
Photovoltaic parameters of DSCs with different transition-metal nitrides and simulated parameters of EIS from CE–CE cells.

| Sample	V_{OC} (V)	J_{SC} (mA cm^{-2})	FF	η (%)	R_S (Ω)	CPE-T (μF)	R_{CT} (Ω)	Z_{W-R} (Ω)	Subgroup in the periodic table	Ref
TiN	796	12.83	0.61	6.23	22.5	68.5	11.2	84.7	IVB	[85]
VN	788	11.74	0.64	5.92	19.6	43.2	9.5	20.7	VB	[85]
CrN	818	10.39	0.64	5.44	18.5	128.9	22.7	234.2	VIB	[85]
ZrN	733	8.2	0.2	1.2	21.3	4.7	420	264.3	IVB	[85]
NbN	798	9.81	0.47	3.68	19.6	81.6	61.5	113.6	VB	[85]
Mo$_2$N	784	11.68	0.66	6.04	19.1	39.4	6.4	152.4	VIB	[85]
Ni$_3$N	766	15.76	0.69	8.31	10.42	1170	13.91	35.39	VIII	[86]
MoN	735	11.55	0.66	5.57	28.4	–	0.8	12.2	VIB	[87]
Fe$_2$N	535	12.20	0.41	2.65	28.9	–	12.11	183.7	VIII	[87]
WN	700	9.75	0.54	3.67	28.4	–	1.11	23.11	VIB	[87]
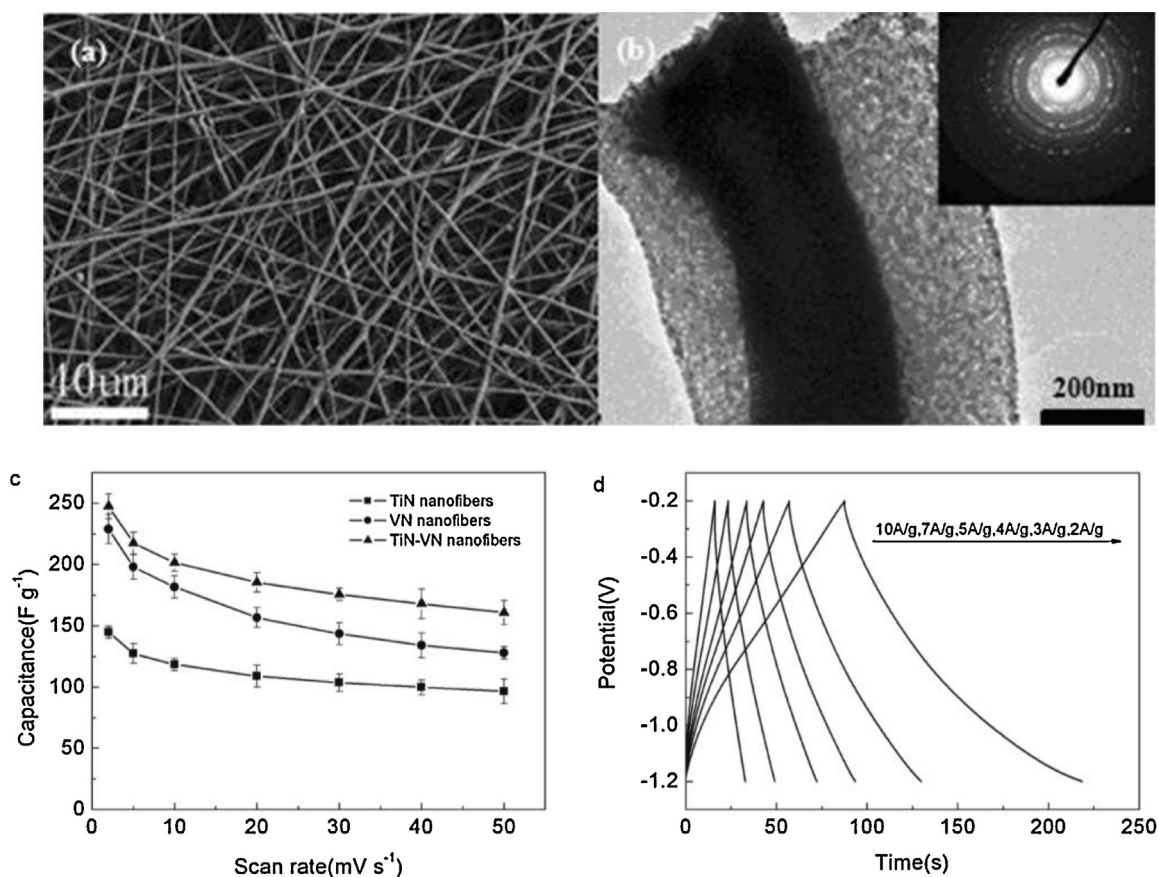
Fig. 9. Typical SEM image (a), TEM image (b) and electrochemical characterization (c and d) of mesoporous coaxial TiN–VN fibers with core–shell structure. Figure was reproduced from Ref. [44], with permission of the copyright holders.

electricity [81–84]. As a typical catalysis for the redox electrolyte (I_3^-/I^-), Pt may limit the potential large scale applications because of the natural scarcity. Recently, various transition-metal nitrides with similar electronic structure and catalyst properties have been proposed for the substitution of the noble metal Pt to break through the bottleneck of DSCs with further industrialization. Table 2 provides a summary of the transition-metal nitrides. Among various studies, Ma et al. systematically studied the electrocatalytic activity of nanoscale early-transition-metal nitride (TiN, ZrN, VN, NbN, CrN and Mo_2N) (Table 2) [85]. It is demonstrated that in order of increasing catalytic activity for the reduction of I_3^- to I^- in the electrolyte, they are $ZrN < NbN < CrN < TiN < VN < Mo_2N$. However, TiN exhibited the highest power conversion efficiencies of 6.23%, which may attribute to the high V_{OC}.

Nanostructured materials with high electrocatalytic sites are efficient to enhance the catalytic activity, owing to the high electrocatalytic sites. However, transition metal nitrides nanoparticles such as TiN nanoparticles suffered from worse conductivity than bulk materials, owing to grain boundary [86]. To address these issues mentioned above, electronic nanowiring by conductive polymer or carbon coating may be a better alternative, which also endows an efficiently combined network of both high electrical conductivity and superior electrocatalytic activity. The composite films of TiN particles, TiN nanorods and TiN mesoporous spheres in conjunction with PEDOT/PSS as CEs were explored by Cui and co-workers [88]. Among them, the energy conversion efficiency of the cell with TiN(P)-PEDOT:PSS as CE reached 7.06%, which was superior to 6.57% of the cell with Pt-FTO under the same experimental condition. On the other hand, TiN–CNTs [89], TiN-conductive carbon black composite [90,91] and TiN/nitrogen-doped graphene [92], were explored as promising alternative for highly efficient

and low-cost CEs for DSCs. When TiN nanoparticles were dispersed on an efficient electron transport network, the hybrids can possess simultaneously mixed conducting network and optimized electrocatalytic properties, which are crucial for high performance DSC.

Furthermore, the high light reflectivity is essential for well-operating CE to improve light harvesting efficiency of DSCs [93]. Right promoted by this expectation, Cui et al. prepared hierarchical micro/nano-structured TiN spheres (micro/nano-TiNs) with tunable sizes and evaluated their effect on the cell performance (Fig. 3), where nanoscale particles provided abundant catalytic active sites while the large microscale particles improved the light-harvesting efficiency. Ultimately, the big submicroscale particles of 800 nm achieved the best results as mentioned above with J_{SC} of 16.57 mA cm^{-2}, V_{OC} of 759 mV, FF of 62% and a η of 7.83%.

4.2. Transition metal nitrides for the electrochemical catalysis of oxygen in air electrodes

For fuel cell and Li-air batteries applications, electrode materials are involved as electrocatalysts for oxygen. Therefore, similar to catalysis of I_3^-/I^-, both excellent catalytic activity and electronic conductivity are required for the mixed conducting electrodes. The catalysis reaction at the hybrid electrolyte (aqueous/non-aqueous) Li-air cathode is similar to that in a fuel cell system. Therefore, platinum-based materials have exhibited the best overall performance for electrocatalysis. However, in aprotic electrolyte, noble metal materials can form an insensitive surface layer during operation by catalyzing the decomposing of organic electrolyte [94,95]. In addition, the prohibitive cost of noble metal material limits its large-scale commercialization. Therefore, the material scientists have devoted considerable efforts to explore highly efficient
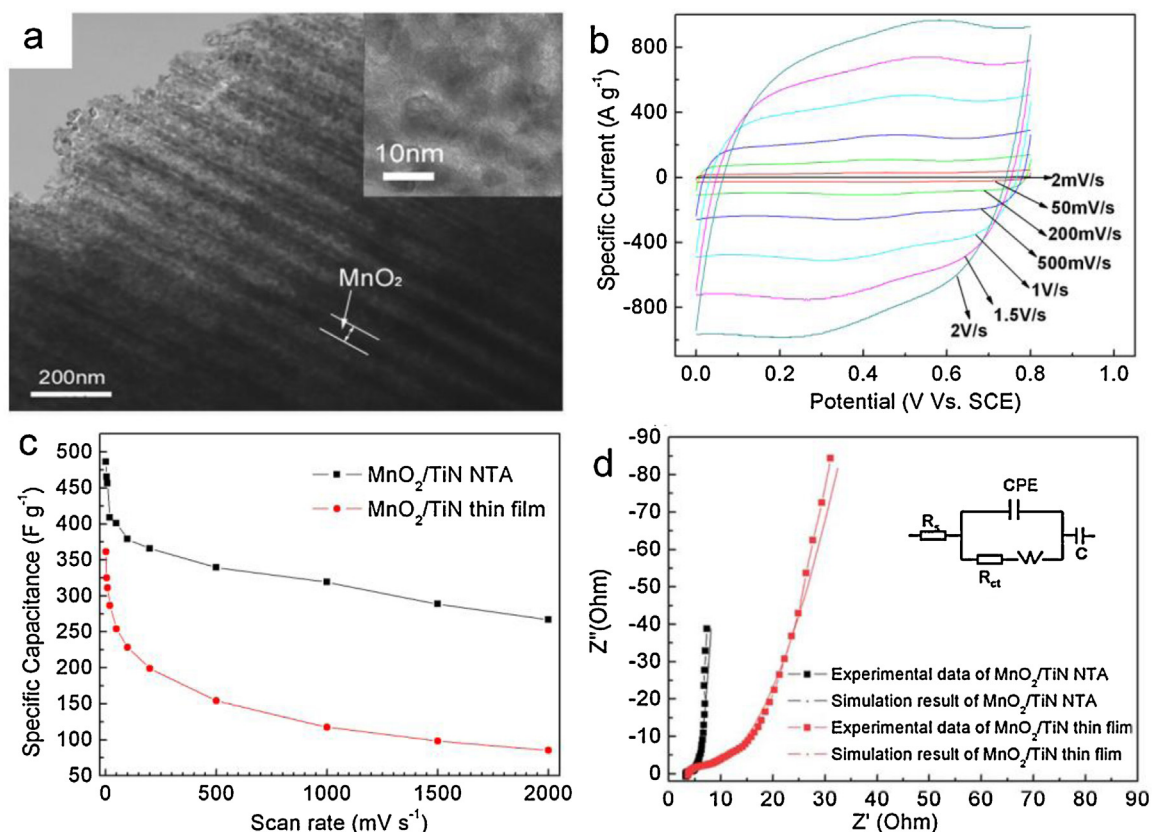
Fig. 10. (a) TEM image of the coaxial MnO$_2$/TiN; (b) rate-dependent cyclic voltammograms of MnO$_2$/TiN NTA electrodes at various scan rates from 2 to 2000 mV s^{-1}; (c) the specific capacitance obtained from MnO$_2$/TiN NTA electrodes (black) and MnO$_2$/TiN thin film electrodes as a function of scan rates; (d) EIS plots for MnO$_2$/TiN NTA (black) and MnO$_2$/TiN thin film electrodes (red), and their corresponding simulation results.
Figure was reproduced from Ref. [46], with permission of the copyright holders.

non-noble metal catalysts. As for the applications of transition metal nitrides, recently, MoN exhibiting high Pt-like electrocatalytic activities, has attracted research attention [96,97]. TiN with excellent electronic conductivity has also been explored for electrochemical catalysis of oxygen reduction reactions (ORR) [98,99]. In 2011, Zhou et al. firstly reported the application of TiN materials as the air electrodes for hybrid electrolyte Li-air batteries [99]. A high ORR cathodic current was observed at an onset potential of 3.80 V vs. Li/Li$^+$. The single cell exhibited a discharge curve with a voltage plateau of 2.85 V at the current density of 0.5 mA g^{-1}.

Nanostructured materials may offer additional advantages for electrocatalysis, as these materials can offer a favorable access of electrolyte to the reactive sites, promoting the mass transfer of the reactant gas and ions conducting in the catalyst layer. Chen
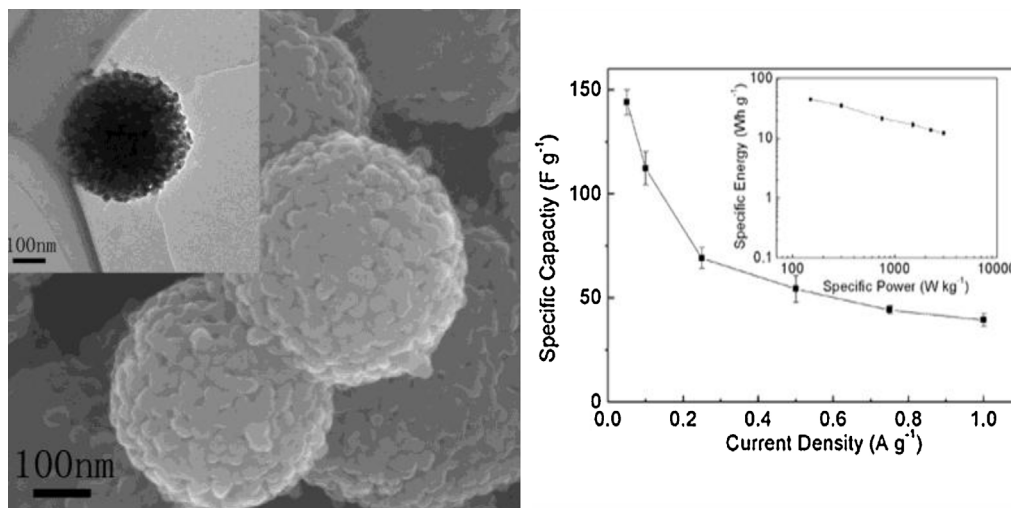

Fig. 11. (a) SEM image and TEM image (inset) of the mesoporous TiN spheres with diameter range from 200 to 300 nm; (b) single-electrode capacitance of TiN mesoporous spheres symmetric supercapacitor as a function of charge/discharge current density and the Ragone plot of TiN-2 symmetric supercapacitor (inset).
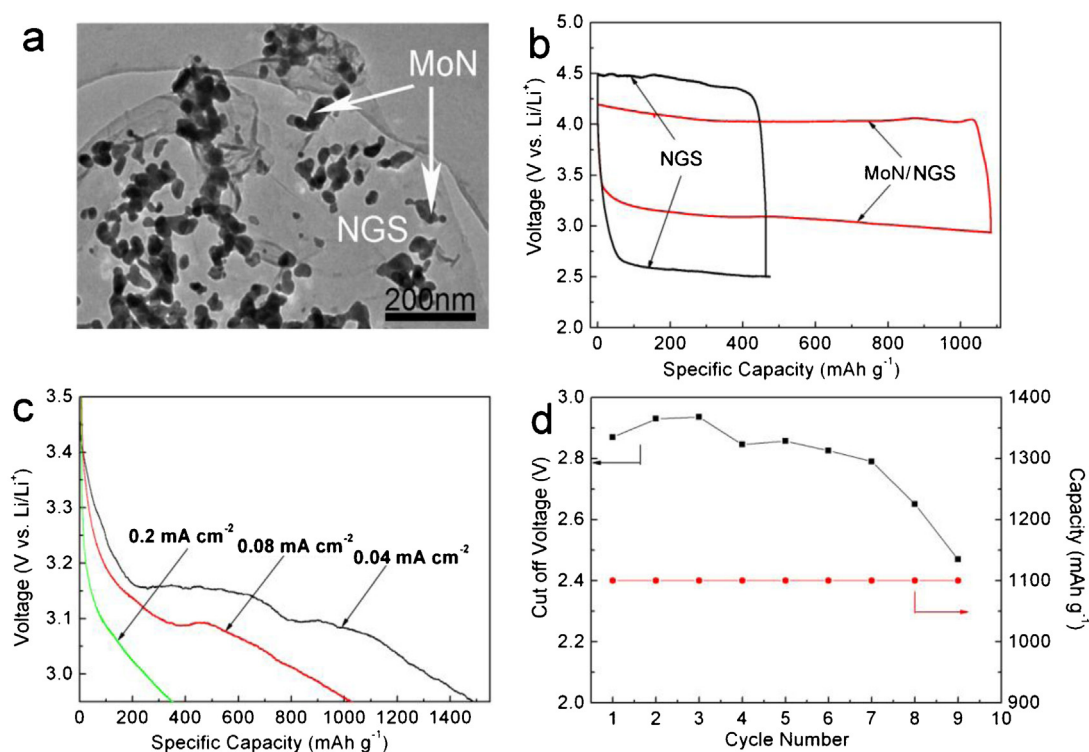Figure was reproduced from Ref. [43], with permission of the copyright holders.

Fig. 12. (a) TEM images of MoN/NGS; (b) discharge/charge curves of MoN/NGS and NGS at the current density of 0.08 mA cm^{-2}; (c) discharge/charge curves of MoN/NGS at different current densities; (d) cycle performance of MoN/NGS cathode based Li-O$_2$ batteries with restricting the capacity to 1100 mAh g^{-1} at a current density of 0.08 mA cm^{-2} (red) and the cut off voltage of discharge, correspondingly (black).

Figure was reproduced from Ref. [99], with permission of the copyright holders.

and co-workers reported a facile preparation of Cu$_3$N nanocubes with a tunable size, which delivered promising electrocatalytic activity toward oxygen reduction [100]. Antonietti et al. [98], have reported a direct synthesis of TiN nanoparticles on carbon black supports using mpg-C$_3$N$_4$/CB composite as a template, which ensured improved contact between electrocatalyst (TiN) and carbon supports. This nanocomposite can function as an efficient cathode catalyst for oxygen reduction reaction in polymer electrolyte fuel cell.

The fundamental understanding of oxygen catalysis in aprotic electrolyte is one of the most challenging tasks in developing non-aqueous Li-air batteries. According to Maier et al. [95], a noble metal catalyst, such as Au, Pt, may strongly catalyze organic solvent molecules to form a passivated layer, which may decrease its ORR activity for non-aqueous Li-air batteries. As a non-noble metal candidate, a hybrid nanostructured material of molybdenum nitride/nitrogen-doped graphene nanosheets (MoN/NGS) was designed by our group and explored as an O$_2$ cathode (Fig. 12) [101]. MoN was synthesized in situ and evenly coated on nitrogen-doped graphene nanosheets, which typically possessed large surface areas and good electronic conductivity. The hybrid nanocomposite exhibits a high discharge plateau at around 3.1 V and a large specific capacity of 1050 mA h g^{-1}. The round-trip efficiency of 77% in our case was the same as that of a PtAu/C cathode. Up to date, the application of transition metal nitrides for non-aqueous Li-air batteries air electrode are still quite limited. The further studies of these materials will definitely provide some clues on how to design a high efficient electrocatalyst for non-aqueous Li-air batteries.

5. Summary

In summary, we present a brief review on the preparation and application of nanostructured transition metal nitrides. Due to their interesting electronic structure, superior hardness, and corrosion resistance, transition metal nitrides has drawn widely scientific attention as an attractive alternative for the electrode materials of electrochemical systems. Furthermore, the concept of mixed (both ionic and electronic) conducting networks has been emphasized in this review, which refers to the material design for achieving enhanced performance of electrode in electrochemical devices. We have tried to include the most important researches in this review. However, this article is unable to list all the exciting works in this field, due to the tremendous explorations in various applications and the rapid pace of researches on nanostructured transition metal nitrides. Driven by the exciting scientific challenges, the studies of in this field has great potential to offer a strong impetus to the applications of electrochemical energy storage and conversion devices.

References

[1] D.P. Thompson, Digital Encyclopedia of Applied Physics, Wiley, New York, 2003.
[2] E. Zintl, G. Brauer, Zeit. Electrochem. 41 (1935) 102.
[3] U.V. Alpen, A. Rabenau, G.H. Talat, Appl. Phys. Lett. 30 (1977) 621.
[4] S. Wild, P. Grieveson, K.H. Jack, in: P. Popper (Ed.), Special Ceramics, British Ceramic Research Association, Stoke-on-Trent, 1972.
[5] S.V. Didziulis, K.D. Butcher, S.S. Perry, Inorg. Chem. 42 (2003) 7766.

[6] H.W. Hugosson, O. Eriksson, U. Jansson, A.V. Ruban, P. Souvatzis, I.A. Abrikosov, Surf. Sci. 557 (2004) 243.
[7] J.-L. Calais, Adv. Phys. 26 (1977) 847.
[8] A. Neckel, Int. J. Quantum Chem. 23 (1983) 1317.
[9] K. Schwarz, CRC Crit. Rev. Solid State Mater. Sci. 13 (1987) 11.
[10] E. Siegel, Semicond. Insul. 5 (1979) 47.
[11] S.T. Oyama, Catal. Today 15 (1992) 179.
[12] S.A. Jansen, R. Hoffmann, Surf. Sci. 197 (1988) 474.
[13] L.E. Toth, Transition Metal Carbides and Nitrides, Academic Press, New York, London, 1971.
[14] J.G. Chen, Chem. Rev. 96 (1996) 1477.
[15] J. Maier, in: B.E. Conway, C.G. Vayenas, R.E. White (Eds.), Modern Aspects of Electrochemistry, Kluwer Academic/Plenum Publishers, 2005.
[16] J. Maier, in: C.G. Vayenas (Ed.), Modern Aspects of Electrochemistry, Kluwer Academic/Plenum Press, New York, 2007.
[17] J. Maier, J. Power Sources 174 (2007) 569.
[18] Y.-G. Guo, J.-S. Hu, L.-J. Wan, Adv. Mater. 20 (2008) 2878.
[19] Y.S. Hu, L. Kienle, Y.G. Guo, J. Maier, Adv. Mater. 18 (2006) 1421.
[20] H. Li, L.H. Shi, Q. Wang, L.Q. Chen, X.J. Huang, Solid State Ionics 148 (2002) 247.
[21] Y.-G. Guo, Y.-S. Hu, W. Sigle, J. Maier, Adv. Mater. 19 (2007) 2087.
[22] C. Giordano, M. Antonietti, Nano Today 6 (2011) 366.
[23] R.A. Andrievski, J. Mater. Sci. 32 (1997) 4463.
[24] S. Komiya, K. Tsuruoka, J. Vacuum Sci. Technol. 13 (1976) 520.
[25] P. Schaaf, M. Kahle, E. Carpene, Appl. Surf. Sci. 247 (2005) 607.
[26] G. Vissokov, I. Grancharov, T. Tsvetanov, Plasma Sci. Technol. 5 (2003) 2039.
[27] H. Moureu, C.H. Hamblet, J. Am. Chem. Soc. 59 (1937) 33.
[28] Z. Zhang, R. Liu, Y. Qian, Mater. Res. Bull. 37 (2002) 1005.
[29] L. Volpe, M. Boudart, J. Solid State Chem. 59 (1985) 332.
[30] W. Yao, P. Makowski, C. Giordano, F. Goettmann, Chem. Eur. J. 15 (2009) 11999.
[31] J. Buha, I. Djerdj, M. Antonietti, M. Niederberger, Chem. Mater. 19 (2007) 3499.
[32] D. Choi, P.N. Kumta, J. Am. Ceram. Soc. 90 (2007) 3113.
[33] D. Choi, P.N. Kumta, Electrochem. Solid-State Lett. 8 (2005) A418.
[34] D. Choi, P.N. Kumta, J. Electrochem. Soc. 153 (2006) A2298.
[35] A. Fischer, M. Antonietti, A. Thomas, Adv. Mater. 19 (2007) 264.
[36] C. Giordano, C. Erpen, W. Yao, B. Milke, M. Antonietti, Chem. Mater. 21 (2009) 5136.
[37] A. Fischer, J.O. Muller, M. Antonietti, A. Thomas, ACS Nano 2 (2008) 2489.
[38] Y. Jun, W.H. Hong, M. Antonietti, A. Thomas, Adv. Mater. 21 (2009) 4270.
[39] B.M. Gray, S. Hassan, A.L. Hector, A. Kalaji, B. Mazumder, Chem. Mater. 21 (2009) 4210.
[40] T. Yu, Y. Deng, L. Wang, R. Liu, L. Zhang, B. Tu, D. Zhao, Adv. Mater. 19 (2007) 2301.
[41] A. Fischer, Y. Jun, A. Thomas, M. Antonietti, Chem. Mater. 20 (2008) 7383.
[42] K. Bang, S. Suslick, Adv. Mater. 21 (2009) 3186.
[43] S. Dong, X. Chen, L. Gu, X. Zhou, H. Xu, H. Wang, Z. Liu, P. Han, J. Yao, L. Wang, G. Cui, L. Chen, ACS Appl. Mater. Inter. 3 (2011) 93.
[44] X. Zhou, C. Shang, L. Gu, S. Dong, X. Chen, P. Han, L. Li, J. Yao, Z. Liu, H. Xu, Y. Zhu, G. Cui, ACS Appl. Mater. Inter. 3 (2011) 3058.
[45] S. Dong, X. Chen, L. Gu, L. Zhang, X. Zhou, Z. Liu, P. Han, H. Xu, J. Yao, X. Zhang, L. Li, C. Shang, G. Cui, Biosens. Bioelectron. 26 (2011) 4088.
[46] S. Dong, X. Chen, L. Gu, X. Zhou, L. Li, Z. Liu, P. Han, H. Xu, J. Yao, H. Wang, X. Zhang, C. Shang, G. Cui, L. Chen, Energy Environ. Sci. 4 (2011) 3502.
[47] S.W. Lee, B.M. Gallant, H.R. Byon, P.T. Hammond, S.-H. Yang, Energy Environ. Sci. 4 (2011) 1972.
[48] D. Howell, Progress Report for Energy Storage Research and Development, U.S. Department of Energy, 2008.
[49] USABC, Requirements of End of Life Energy Storage Systems for PHEVs <http://www.uscar.org>.
[50] Y. Idota, T. Kubota, A. Matsufuji, Y. Maekawa, T. Miyasaka, Science 276 (1997) 1395.
[51] P. Poizot, S. Laruelle, S. Grugeon, L. Dupont, J.M. Tarascon, Nature 407 (2000) 496.
[52] J. Cabana, L. Monconduit, D. Larcher, M.R. Palacín, Adv. Mater. 22 (2010) E170.
[53] J.B. Bates, N.J. Dudney, B. Neudecker, A. Ueda, C.D. Evans, Solid State Ionics 135 (2000) 33.
[54] N. Pereira, L.C. Klein, G.G. Amatucci, J. Electrochem. Soc. 149 (2002) A262.
[55] N. Pereira, L. Dupont, J.M. Tarascon, L.C. Klein, G.G. Amatucci, J. Electrochem. Soc. 150 (2003) A1273.
[56] Q. Sun, Z.-W. Fu, Electrochem. Solid-State Lett. 10 (2007) A189.
[57] Y. Wang, Z-W. Fu, X-L. Yue, Q-Z. Qin, J. Electrochem. Soc. 151 (2004) E162.
[58] Z-W. Fu, Y. Wang, X-L. Yue, S-L. Zhao, Q-Z. Qin, J. Phys. Chem. B 108 (2004) 2236.
[59] C-X. Zu, H. Li, Energy Environ. Sci. 4 (2011) 2614.
[60] K. Zhang, H. Wang, X. He, Z. Liu, L. Wang, L. Gu, H. Xu, P. Han, S. Dong, C. Zhang, J. Yao, G. Cui, L. Chen, J. Mater. Chem. 21 (2011) 11916.
[61] W. Lengauer, A. Eder, Encyclopedia of Inorganic Chemistry, John Wiley & Sons Ltd., 2006.
[62] G. Cui, L. Gu, A. Thomas, L. Fu, P.A. van Aken, M. Antonietti, J. Maier, ChemPhysChem 11 (2010) 3219.
[63] Y. Yue, P. Han, X. He, K. Zhang, Z. Liu, C. Zhang, S. Dong, L. Gu, G. Cui, J. Mater. Chem. 22 (2012) 4938.
[64] Q. Sun, Z-W. Fu, Appl. Surf. Sci. 258 (2012) 3197.
[65] Y. Wang, W-Y. Liu, Z-W. Fu, Acta Phys. Chim. Sin. 22 (2006) 65.
[66] B. Das, M.V. Reddy, P. Malar, Thomas Osipowicz, G.V. Subba Rao, B.V.R. Chowdari, Solid State Ionics 180 (2009) 1061.
[67] D. Choi, G.E. Blomgren, P.N. Kumta, Adv. Mater. 18 (2006) 1178.
[68] P.J. Hanumantha, P.N. Kumta, 218th ECS Meeting of The Electrochemical Society, 2010.
[69] X. Zhou, H. Chen, D. Shu, C. He, J. Nan, J. Phys. Chem. Solids 70 (2009) 495.
[70] A.M. Glushenkov, D. Hulicova-Jurcakova, D. Llewellyn, G.Q. Lu, Y. Chen, Chem. Mater. 22 (2010) 914.
[71] L. Zhang, C.M.B. Holt, E.J. Luber, B.C. Olsen, H. Wang, M. Danaie, X. Cui, X. Tan, V.W. Lui, W.P. Kalisvaart, D. Mitlin, J. Phys. Chem. C 115 (2011) 24381.
[72] S. Dong, X. Chen, L. Gu, X. Zhou, H. Wang, Z. Liu, P. Han, J. Yao, L. Wang, G. Cui, L. Chen, Mater. Res. Bull. 46 (2011) 835.
[73] D. Choi, P.N. Kumta, J. Am. Chem. Soc. 90 (2007) 3113.
[74] C.Z. Deng, R.A.J. Pynenberg, K.C. Tsai, J. Electrochem. Soc. 145 (1998) L61.
[75] C. Chen, D. Zhao, D. Xu, X. Wang, Mater. Chem. Phys. 95 (2006) 84.
[76] K. Naoi, Fuel cells 10 (2010) 825.
[77] K. Naoi, S. Ishimoto, Y. Isobe, S. Aoyagi, J. Power Sources 195 (2010) 6250.
[78] J.-H. Kim, J.-S. Kim, Y.-G. Lim, J.-G. Lee, Y.-J. Kim, J. Power Sources 196 (2011) 10490.
[79] V. Khomenko, E. Raymundo-Pinero, F. Beguin, J. Power Sources 177 (2008) 643.
[80] B.Z. Jang, C. Liu, D. Neff, Z. Yu, M.C. Wang, W. Xiong, A. Zhamu, Nano Lett. 11 (2011) 3785.
[81] B. Oregan, M. Gratzel, Nature 353 (1991) 737.
[82] M.K. Nazeeruddin, A. Kay, I. Rodicio, R. Humphrybaker, E. Muller, P. Liska, N. Vlachopoulos, M. Gratzel, J. Am. Chem. Soc. 115 (1993) 6382.
[83] M. Gratzel, J. Photochem. Photobiol. A 164 (2004) 3.
[84] M. Gratzel, Inorg. Chem. 44 (2005) 6841.
[85] M. Wu, X. Lin, Y. Wang, L. Wang, W. Guo, D. Qu, X. Peng, A. Hagfeldt, M. Graetzel, T. Ma, J. Am. Chem. Soc. 134 (2012) 3419.
[86] Q.W. Jiang, G.R. Li, X.P. Gao, Chem. Commun. (2009) 7603.
[87] G.R. Li, J. Song, G.L. Pan, X.P. Gao, Energy Environ. Sci. 4 (2011) 1680.
[88] H. Xu, X. Zhang, C. Zhang, Z. Liu, X. Zhou, S. Pang, X. Chen, S. Dong, Z. Zhang, L. Zhang, P. Han, X. Wang, G. Cui, ACS Appl. Mater. Inter. 4 (2012) 1087.
[89] G.R. Li, F. Wang, Q.W. Jiang, X.P. Gao, P.W. Shen, Angew. Chem. Int. Ed. 49 (2010) 3653.
[90] G.R. Li, F. Wang, J. Song, F.Y. Xiong, X.P. Gao, Electrochim. Acta 65 (2012) 216.
[91] E. Ramasamy, C. Jo, A. Anthonysamy, I. Jeong, J.K. Kim, J. Lee, Chem. Mater. 24 (2012) 1575.
[92] Z. Wen, S. Cui, H. Pu, S. Mao, K. Yu, X. Feng, J. Chen, Adv. Mater. 23 (2011) 5445.
[93] X.M. Fang, T.L. Ma, G.Q. Guan, M. Akiyama, T. Kida, E. Abe, J. Electroanal. Chem. 570 (2004) 257.
[94] Y.-C. Lu, H.A. Gasteiger, E. Crumlin, R. McGuire, S.-H. Yang, J. Electrochem. Soc. 157 (2010) A1016.
[95] S. Hore, G. Kaiser, Y.-S. Hu, A. Schulz, M. Konuma, G. Gotz, W. Sigle, A. Verhoeven, J. Maier, J. Mater. Chem. 18 (2008) 5589.
[96] D. Xia, S. Liu, Z. Wang, G. Chen, L. Zhang, L. Zhang, S. Hui, J. Zhang, J. Power Sources 177 (2008) 296.
[97] J. Qi, L. Jiang, Q. Jiang, S. Wang, G. Sun, J. Phys. Chem. C 114 (2010) 18159.
[98] J. Chen, K. Takanabe, R. Ohnishi, D. Lu, S. Okada, H. Hatasawa, H. Morioka, M. Antonietti, I. Kubota, K. Domen, Chem. Commun. 46 (2010) 7492.
[99] P. He, Y. Wang, H. Zhou, Chem. Commun. 47 (2011) 10701.
[100] H. Wu, W. Chen, J. Am. Chem. Soc. 133 (2011) 15236.
[101] S. Dong, X. Chen, K. Zhang, L. Gu, L. Zhang, X. Zhou, L. Li, Z. Liu, P. Han, H. Xu, J. Yao, C. Zhang, X. Zhang, C. Shang, G. Cui, L. Chen, Chem. Commun. 47 (2011) 11291.